Photometric method for determining surface orientation from multiple images

Robert J. Woodham

Department of Computer Science
University of British Columbia
2075 Wesbrook Mall
Vancouver, B.C., Canada
V6T 1W5

Abstract. A novel technique called photometric stereo is introduced. The idea of photometric stereo is to vary the direction of incident illumination between successive images, while holding the viewing direction constant. It is shown that this provides sufficient information to determine surface orientation at each image point. Since the imaging geometry is not changed, the correspondence between image points is known *a priori*. The technique is photometric because it uses the radiance values recorded at a single image location, in successive views, rather than the relative positions of displaced features.

Photometric stereo is used in computer-based image understanding. It can be applied in two ways. First, it is a general technique for determining surface orientation at each image point. Second, it is a technique for determining object points that have a particular surface orientation. These applications are illustrated using synthesized examples.

I. INTRODUCTION

Work on computer-based image understanding has led to a need to model the imaging process. One aspect of this concerns the geometry of image projection. Less well understood is the radiometry of image formation. Relating the radiance values recorded in an image to object shape requires a model of the way surfaces reflect light.

A reflectance map is a convenient way to incorporate a fixed scene illumination, surface reflectance and imaging geometry into a single model that allows image intensity to be written as a function of surface orientation. This function is not invertible since surface orientation has two degrees of freedom and image intensity provides only one measurement. Local surface shape cannot, in general, be determined from the intensity value recorded at a single image point. In order to determine object shape, additional information must be provided.

This observation has led to a novel technique called photometric stereo in which surface orientation is determined from two or more images. Traditional stereo techniques determine range by relating two images of an object viewed from different directions. If the correspondence between picture elements is known, then distance to the object can be calculated by triangulation. Unfortunately, it is difficult to determine this correspondence. The idea of photometric stereo is to vary the direction of the incident illumination between successive images, while holding the viewing direction constant. It is shown that this provides sufficient information to determine surface orientation at each image point. Since the imaging geometry is not changed, the correspondence between image points is known *a priori*. The technique is photometric because it uses the radiance values recorded at a single image location, in successive views, rather than the relative positions of displaced features.

II. THE REFLECTANCE MAP

The fraction of light reflected by an object surface in a given direction depends upon the optical properties of the surface material, the surface microstructure and the spatial and spectral distribution and state of polarization of the incident illumination. For many surfaces, the fraction of the incident illumination reflected in a particular direction depends only on the surface orientation. The reflectance characteristics of such a surface can be represented as a function $\phi(i,e,g)$ of the three angles i, e and g defined in Figure 1. These are called, respectively, the *incident*, *emergent* and *phase* angles. The angles i and e are defined relative to a local surface normal. $\phi(i,e,g)$ determines the ratio of surface radiance to irradiance measured per unit surface area, per unit solid angle, in the direction of the viewer. The reflectance function $\phi(i,e,g)$ defined here is related to the bidirectional reflectance distribution function (BRDF) defined by the National Bureau of Standards.[1]

Image forming systems perform a perspective transformation, as illustrated in Figure 2(a). If the size of the objects in view is small compared to the viewing distance, then the perspective projection can be approximated as an orthographic projection, as illustrated in Figure 2(b). Consider an image forming system that performs an orthographic projection. To standardize the imaging geometry, it is convenient to choose a coordinate system such that the viewing direction is aligned with the negative z-axis. Also, assume appropriate scaling of the image plane such that object point (x,y,z) maps onto image point (u,v) where u = x and v = y. With these assumptions, image coordinates (x,y) and object coordinates (x,y) can be referred to interchangeably.

If the equation of an object surface is given explicitly as:

$$z = f(x,y)$$

then a surface normal is given by the vector:

$$\left[\frac{\partial f(x,y)}{\partial x}, \frac{\partial f(x,y)}{\partial y}, -1 \right]$$
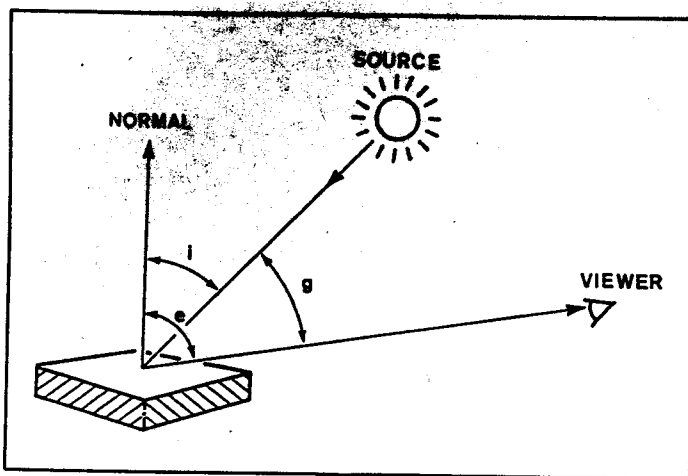
If parameters p and q are defined by:

Figure 1. Defining the three angles i, e and g. The incident angle i is the angle between the incident ray and the surface normal. The emergent angle e is the angle between the emergent ray and the surface normal. The phase angle g is the angle between the incident and emergent rays.
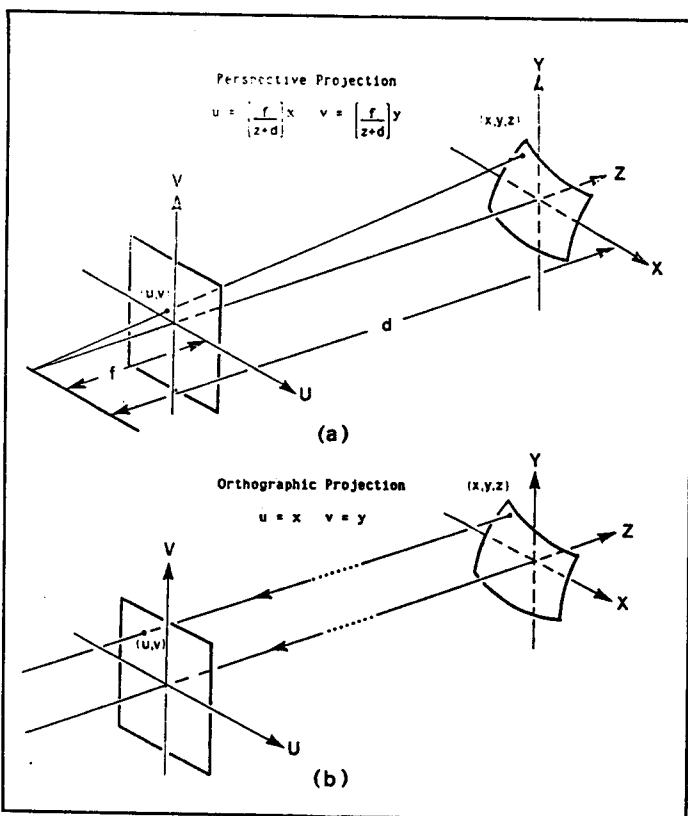

Figure 2. Characterizing image projections. (a) illustrates the well-known perspective projection. [Note: to avoid image inversion, it is convenient to assume that the image plane lies in front of the lens rather than behind it.] For objects that are small relative to the viewing distance, the image projection can be modeled as the orthographic projection illustrated in (b). In an orthographic projection, the focal length f is infinite so that all rays from object to image are parallel.

$$p = \frac{\partial f(x,y)}{\partial x} \quad \text{and} \quad q = \frac{\partial f(x,y)}{\partial y}$$

then the surface normal can be written as $[p,q,-1]$. The quantity (p,q) is called the *gradient* of $f(x,y)$ and *gradient space* is the two-dimensional space of all such points (p,q). Gradient space is a con-

venient way to represent surface orientation. It has been used in scene analysis.[2] In image analysis, it is used to relate the geometry of image projection to the radiometry of image formation.[3] This relation is established by showing that image intensity can be written explicitly as a function of gradient coordinates p and q.

An ideal imaging device produces image irradiances proportional to scene radiances. In an orthographic projection, the viewing direction, and hence the phase angle g, is constant for all object points. Thus, for a fixed light source and viewer geometry, the ratio of scene radiance to irradiance depends only on gradient coordinates p and q. Further, suppose each object surface element receives the same incident radiance. Then, the scene radiance, and hence image intensity, depends only on gradient coordinates p and q.

The *reflectance map* R(p,q) determines image intensity as a function of p and q. A reflectance map captures the surface reflectance of an object material for a particular light source, object surface and viewer geometry. Reflectance maps can be determined empirically, derived from phenomenological models of surface reflectivity or derived from analytic models of surface microstructure.

In this paper, it will be assumed that image projection is orthographic and that incident illumination is given by a single distant point source. Extended sources can be modeled as the superposition of single sources. The reflectance map can be extended to incorporate spatially varying irradiance and perspective. A formal analysis of the relation between the reflectance map and the bidirectional reflectance distribution function (BRDF) has been given.[4]

Expressions for cos(i), cos(e) and cos(g) can be derived using normalized dot products of the surface normal vector $[p,q,-1]$, the vector $[p_s,q_s,-1]$ which points in the direction of the light source and the vector $[0,0,-1]$ which points in the direction of the viewer. One obtains:

$$\cos(i) = \frac{1 + pp_s + qq_s}{\sqrt{1 + p^2 + q^2}\ \sqrt{1 + p_s^2 + q_s^2}}$$

$$\cos(e) = \frac{1}{\sqrt{1 + p^2 + q^2}}$$

$$\cos(g) = \frac{1}{\sqrt{1 + p_s^2 + q_s^2}}.$$

These expressions can be used to transform an arbitrary surface reflectance function $\phi(i,e,g)$ into a reflectance map R(p,q).

One simple idealized model of surface reflectance is given by:

$$\phi_a(i,e,g) = \varrho \cos(i).$$

This reflectance function corresponds to the phenomenological model of a perfectly diffuse (lambertian) surface which appears equally bright from all viewing directions. Here, ϱ is a reflectance factor and the cosine of the incident angle accounts for the foreshortening of the surface as seen from the source. The corresponding reflectance map is given by:

$$R_a(p,q) = \frac{\varrho\,(1 + pp_s + qq_s)}{\sqrt{1 + p^2 + q^2}\ \sqrt{1 + p_s^2 + q_s^2}}.$$

A second reflectance function, similar to that of materials in the maria of the moon and rocky planets, is given by:

$$\phi_b(i,e,g) = \frac{\varrho \cos(i)}{\cos(e)}.$$

This reflectance function corresponds to the phenomenological model of a surface which reflects equal amounts of light in all directions. The cosine of the emergent angle accounts for the foreshortening of the surface as seen from the viewer. The corresponding reflectance map is given by:

$$R_b(p,q) = \frac{\varrho (1 + pp_s + qq_s)}{\sqrt{1 + p_s^2 + q_s^2}}.$$

It is convenient to represent $R(p,q)$ as a series of iso-brightness contours in gradient space. Figure 3 and Figure 4 illustrate the two simple reflectance maps $R_a(p,q)$ and $R_b(p,q)$, defined above, for the case $p_s = 0.7$, $q_s = 0.3$ and $\varrho = 1$.
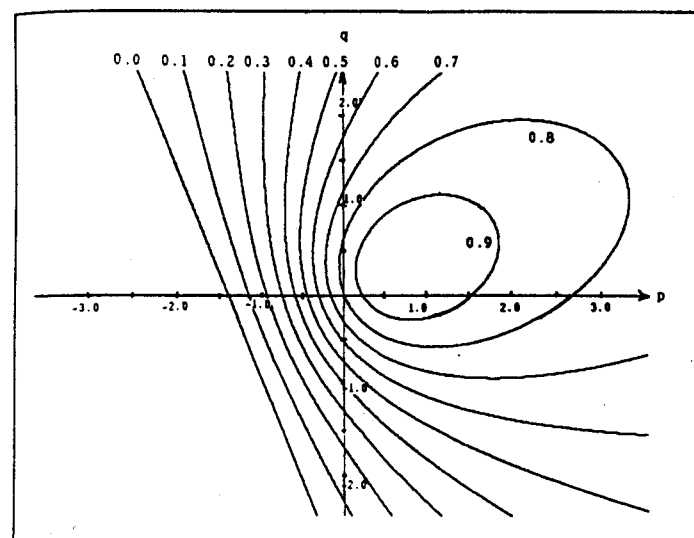

Figure 3. The reflectance map $R_a(p,q)$ for a lambertian surface illuminated from gradient point $p_s = 0.7$ and $q_s = 0.3$ (with $\varrho = 1.0$). The reflectance map is plotted as a series of contours spaced 0.1 units apart.
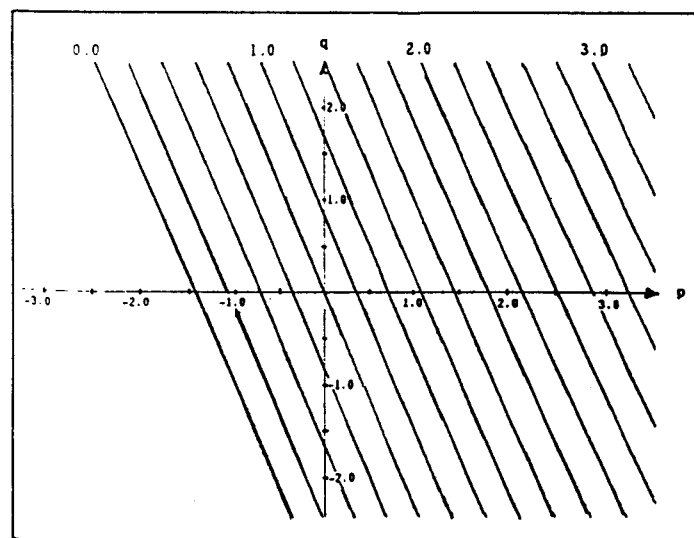

Figure 4. The reflectance map $R_b(p,q)$ for a surface illuminated from gradient point $p_s = 0.7$ and $q_s = 0.3$ (with $\varrho = 1.0$). The reflectance map is plotted as a series of contours spaced 0.2 units apart.

Reflectance map techniques

Using the reflectance map, the basic equation describing the image-forming process can be written as:

$$I(x,y) = R(p,q) . \tag{1}$$

One idea is to use Eq. (1) directly to generate shaded images of surfaces. This has obvious utility in computer graphics applications including hill-shading for automated cartography[5] and video input for a flight simulator.[6] Synthesized imagery can be registered to real imagery to align images with surface models. This technique has been used to achieve precise alignment of Landsat imagery with digital terrain models.[7]

Equation (1) can also be used in image analysis to determine object shape from image intensity. Equation (1) is a nonlinear first-order partial differential equation. Direct solution is tedious.[8] More generally, one can think of Eq. (1) as one equation in the two unknowns p and q. Determining object shape from image intensity is difficult because Eq. (1) is underdetermined. In order to calculate object shape, additional assumptions must be invoked.

Recent work has helped to make these assumptions explicit. For certain materials, such as the material of the maria of the moon, special properties of surface reflectance simplify the solution.[3,8,9] Other methods for determining object shape from image intensity embody assumptions about surface curvature.[3,10] Simple surfaces have been proposed for use in computer aided design.[11] When properties of surface curvature are known *a priori*, they can be exploited in image analysis.[12] This is useful, for example, in industrial inspection since there are often constraints on surface curvature imposed by the drafting techniques available for part design and by the fabrication processes available for part manufacture.[13]

Reflectance map techniques deepen our understanding of what can and cannot be computed directly from image intensity. Photometric stereo is a novel reflectance map technique that uses two or more images to solve Eq. (1) directly.

III. PHOTOMETRIC STEREO

The idea of photometric stereo is to vary the direction of incident illumination between successive views, while holding the viewing direction constant. Suppose two images $I_1(x,y)$ and $I_2(x,y)$ are obtained by varying the direction of incident illumination. Since there has been no change in the imaging geometry, each picture element (x,y) in the two images corresponds to the same object point and hence to the same gradient (p,q). The effect of varying the direction of incident illumination is to change the reflectance map $R(p,q)$ that characterizes the imaging situation.

Let the reflectance maps corresponding to $I_1(x,y)$ and $I_2(x,y)$ be $R_1(p,q)$ and $R_2(p,q)$ respectively. The two views are characterized by two independent equations:

$$I_1(x,y) = R_1(p,q) . \tag{2}$$

$$I_2(x,y) = R_2(p,q) . \tag{3}$$

Two reflectance maps $R_1(p,q)$ and $R_2(p,q)$ are required. But, if the phase angle g is the same in both views (i.e., the direction of illumination is rotated about the viewing direction), then the two reflectance maps are rotations of each other.

For reflectance characterized by $R_b(p,q)$ above, Eqs. (2) and (3) are linear equations in p and q. If the reflectance factor ϱ is known, then two views are sufficient to determine surface orientation at each image point, provided the directions of incident illumination are not collinear in azimuth.

In general, Eqs. (2) and (3) are nonlinear so that more than one solution is possible. One idea would be to obtain a third image:

$$I_3(x,y) = R_3(p,q) \tag{4}$$

to overdetermine the solution.

For reflectance characterized by $R_a(p,q)$ above, three views are sufficient to uniquely determine both the surface orientation and the reflectance factor ϱ at each image point, as will now be shown.[14] Let $\underline{I} = [I_1,I_2,I_3]'$ be the column vector of intensity values recorded at a point (x,y) in each of three views (' denotes vector transpose). Further, let

$$\underline{n}_1 = [n_{11},n_{12},n_{13}]'$$

$$n_2 = [n_{21}, n_{22}, n_{23}]'$$

$$n_3 = [n_{31}, n_{32}, n_{33}]'$$

be unit column vectors defining the three directions of incident illumination. Construct the matrix $\underset{\sim}{N}$ where

$$\underset{\sim}{N} = \begin{bmatrix} n_{11} & n_{12} & n_{13} \\ n_{21} & n_{22} & n_{23} \\ n_{31} & n_{32} & n_{33} \end{bmatrix}$$

Let $\underset{\sim}{n} = [n_1, n_2, n_3]'$ be the column vector corresponding to a unit surface normal at (x,y). Then,

$$\underset{\sim}{I} = \varrho \underset{\sim}{N} \underset{\sim}{n}$$

so that,

$$\varrho \underset{\sim}{n} = \underset{\sim}{N}^{-1} \underset{\sim}{I}$$

provided the inverse $\underset{\sim}{N}^{-1}$ exists. This inverse exists if and only if the three vectors $\underset{\sim}{n}_1$, $\underset{\sim}{n}_2$ and $\underset{\sim}{n}_3$ do not lie in a plane. In this case, the reflectance factor and unit surface normal at (x,y) are given by:

$$\varrho = |\underset{\sim}{N}^{-1} \underset{\sim}{I}|$$

and

$$\underset{\sim}{n} = (1/\varrho)\underset{\sim}{N}^{-1} \underset{\sim}{I} . \tag{5}$$

Unfortunately, since the sun's path across the sky is very nearly planar, this simple solution does not apply to outdoor images taken at different times during the same day.

Even when the simplifications implied by $R_a(p,q)$ and $R_b(p,q)$ above do not hold, photometric stereo is easily implemented. Initial computation is required to determine the reflectance map for each experimental situation. Once calibrated, however, photometric stereo can be reduced to simple table lookup and/or search operations. Photometric stereo is a practical scheme for environments, such as industrial inspection, in which the nature and position of the incident illumination is known or can be controlled.

The multiple images required for photometric stereo can be obtained by explicitly moving a single light source, by using multiple light sources calibrated with respect to each other or by rotating the object surface and imaging hardware together to simulate the effect of moving a single light source. The equivalent of photometric stereo can also be achieved in a single view by using multiple illuminations which can be separated by color.

Applications of photometric stereo

Photometric stereo can be used in two ways. First, photometric stereo is a general technique for determining surface orientation at each image point. For a given image point (x,y), the equations characterizing each image can be combined to determine the corresponding gradient (p,q).

Second, photometric stereo is a general technique for determining object points that have a particular surface orientation. This use of photometric stereo corresponds to interpreting the basic image-forming Eq. (1) as one equation in the unknowns x and y. For a given gradient (p,q), the equations characterizing each image can be combined to determine corresponding object points (x,y). This second use of photometric stereo is appropriate for the so-called industrial "bin-of-parts" problem. The location in an image of key object points is often sufficient to determine the position and orientation of a known object on a table or conveyor belt so that the object may be grasped by an automatic manipulator.

A particularly useful special case concerns object points whose surface normal directly faces the viewer (i.e., object points with $p = 0$ and $q = 0$). Such points form a unique class of image points whose intensity value is invariant under rotation of the illumina-

tion direction about the viewing direction. Object points with surface normal directly facing the viewer can be located without explicitly determining the reflectance map $R(p,q)$. The value of $R(0,0)$ is not changed by varying the direction of illumination, provided only that the phase angle g is held constant.

These applications of photometric stereo will now be illustrated using a simple, synthesized example. Consider a sphere of radius r centered at the object space origin. The explicit representation of this object surface, corresponding to the viewing geometry of Figure 2(b), is given by:

$$z = f(x,y) = -\sqrt{r^2 - x^2 - y^2} . \tag{6}$$

The gradient coordinates p and q are determined by differentiating Eq. (6) with respect to x and y. One finds:

$$p = \frac{-x}{z} \text{ and } q = \frac{-y}{z}$$

Suppose that the sphere is made of a perfectly diffusing object material and is illuminated by a single distant point source at gradient point (p_s, q_s). Then, the reflectance map is given by $R_a(p,q)$ above so that the corresponding synthesized image is:

$$I(x,y) = \begin{cases} 0 & \text{if } x^2 + y^2 > r^2 \\ \max(0, R_a(-x/z, -y/z)) & \text{otherwise} \end{cases} \tag{7}$$

Equation (7) generates image intensities in the range 0 to ϱ. In the example below, r = 60 and $\varrho = 1$.

Multiple images are obtained by varying the position of the light source. Consider three different positions. Let the first be $p_s = 0.7$ and $q_s = 0.3$ as in Figure 3. Let the second and third correspond to rotations of the light source about the viewing direction of −120° and +120° respectively (i.e., $p_s = -0.610$, $q_s = 0.456$ and $p_s = -0.090$, $q_s = -0.756$). Let the three reflectance maps be $R_1(p,q)$, $R_2(p,q)$ and $R_3(p,q)$. The phase angle g is constant in each case. Let the corresponding images generated by Eq. (6) be $I_1(x,y)$, $I_2(x,y)$ and $I_3(x,y)$.

First, consider image point x = 15, y = 20. Here, $I_1(x,y) = 0.942$, $I_2(x,y) = 0.723$ and $I_3(x,y) = 0.505$. Figure 5 illustrates the reflectance map contours $R_1(p,q) = 0.942$, $R_2(p,q) = 0.723$ and $R_3(p,q) = 0.505$. The point p = 0.275, q = 0.367 at which these three contours intersect determines the gradient corresponding to
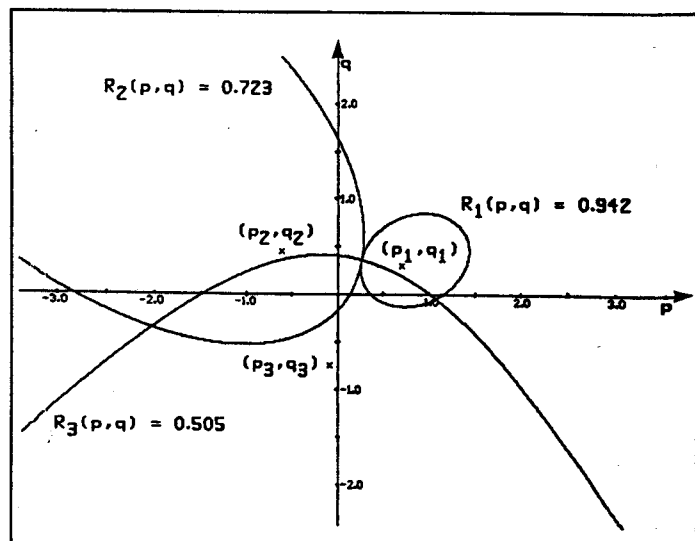
Figure 5. Determining the surface orientation (p,q) at a given image point (x,y). Three reflectance map contours are intersected where each contour corresponds to the intensity value at (x,y) obtained from three separate images. $I_1(x,y) = 0.942$, $I_2(x,y) = 0.723$ and $I_3(x,y) = 0.505$.
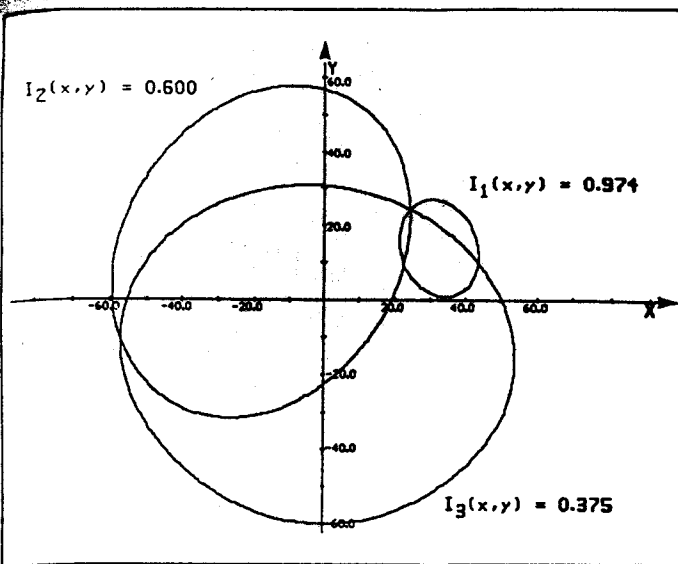
Figure 6. Determining image points (x,y) whose surface orientation is a given (p,q). Three image intensity contours are intersected where each contour corresponds to the value at (p,q) obtained from three separate reflectance maps. $R_1(p,q) = 0.974$, $R_2(p,q) = 0.600$ and $R_3(p,q) = 0.375$.
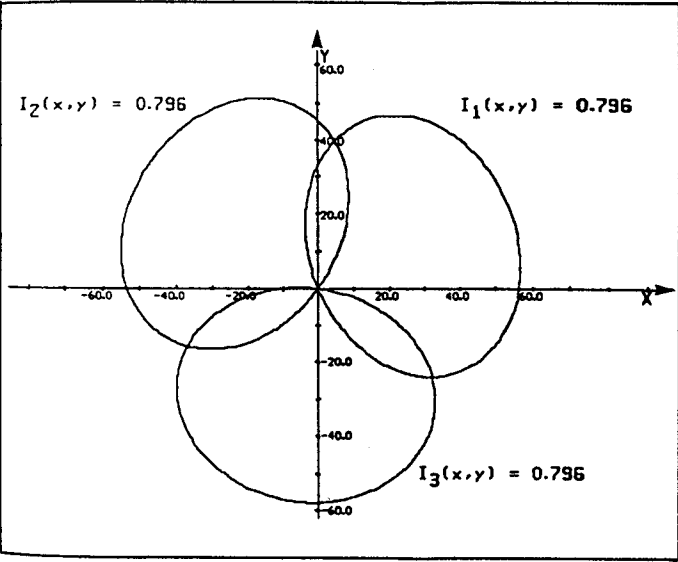

Figure 7. Determining image points (x,y) whose surface normal directly faces the viewer. Three image intensity contours are intersected where each contour corresponds to the value at (0,0) obtained from three separate reflectance maps. Note that the reflectance map value at (0,0) does not change with light source position, provided the phase angle g is held constant.

image point $x = 15$, $y = 20$.

Second, consider gradient point $p = 0.5$, $q = 0.5$. Here, $R_1(p,q) = 0.974$, $R_2(p,q) = 0.600$ and $R_3(p,q) = 0.375$. Figure 6 illustrates the image intensity contours $I_1(x,y) = 0.974$, $I_2(x,y) = 0.600$ and $I_3(x,y) = 0.375$. The point $x = 24.5$, $y = 24.5$ at which these three contours intersect determines an object point whose gradient is $p = 0.5$, $q = 0.5$.

Finally, Figure 7 repeats the example given in Figure 6 but for the case $p = 0$, $q = 0$. Here, $R_1(p,q) = R_2(p,q) = R_3(p,q) = 0.796$. Object points with surface normal directly facing the viewer form a unique class of points whose image intensity is invariant for rotations of the light source about the viewing direction. The point $x = 0$, $y = 0$ at which these three contours intersect determines an object point with surface normal directly

facing the viewer. This result would hold even if the form of $R(p,q)$ is unknown.

Accuracy considerations

Photometric stereo is most accurate in regions of gradient space where the density of reflectance map contours is great and where the contours to be intersected are nearly perpendicular. Several factors influence the density and direction of reflectance map contours. The reflectance properties of the surface material play a role. Figures 3 and 4 illustrate the difference between two idealized materials viewed under identical conditions of illumination. In general, increasing the specular component of reflection will increase the density of contours in one region of gradient space at the expense of other regions. Using extended light sources rather than point sources will alter the shape and distribution of reflectance map contours. Imaging systems can be configured to exploit these facts.[15]

For a given surface material, the main determiner of accuracy is the choice of phase angle g. In photometric stereo, there is a trade-off to acknowledge. A large phase angle increases the density of reflectance map contours in illuminated portions of gradient space. At the same time, a large phase angle results in more of gradient space lying in shadow. A practical compromise must be arrived at for each application.

The relative positions of the light sources must also be considered. Figures 8 and 9 give some indication of the trade-off associated with light source position. In each case, reflectance is
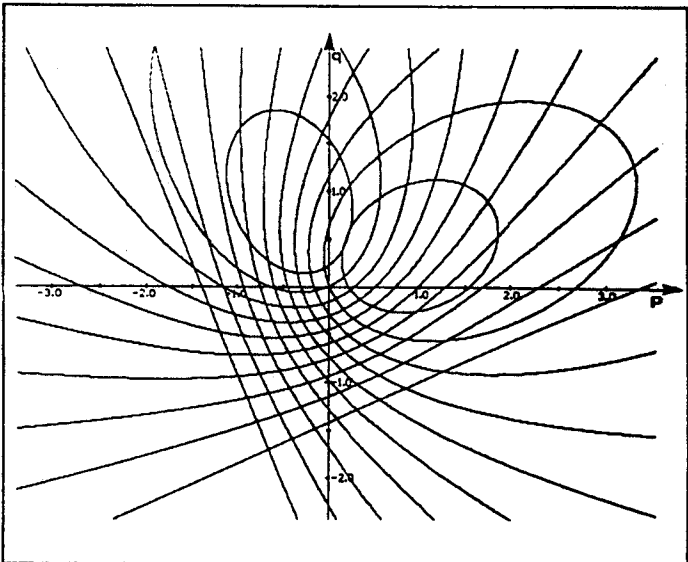

Figure 8. Superimposed reflectance maps $R_1(p,q)$ and $R_2(p,q)$ where $R_1(p,q)$ is $R_a(p,q)$ with $p_s = 0.7$, $q_s = 0.3$, $\varrho = 1$ and $R_2(p,q)$ is $R_a(p,q)$ with $p_s = -0.3$, $q_s = 0.7$, $\varrho = 1$. Each region indicates how an error in intensity measurement determines a corresponding error in the estimation of surface gradient (p,q).

assumed to be characterized by $R_a(p,q)$ above. Figure 8 considers a two-source configuration in which the light source directions are separated by 90° in azimuth with respect to the viewer. Figure 8 superimposes reflectance map contours, spaced 0.1 units apart, for $R_1(p,q)$ and $R_2(p,q)$ where $R_1(p,q)$ is $R_a(p,q)$ with $p_s = 0.7$ $q_s = 0.3$ $\varrho = 1$ and $R_2(p,q)$ is $R_a(p,q)$ with $p_s = -0.3$ $q_s = 0.7$ $\varrho = 1$. Each region of Figure 8 corresponds to a region of equal measurement error. For example, if $I_1(x,y)$ is determined to lie between 0.4 and 0.5 and $I_2(x,y)$ is determined to lie between 0.5 and 0.6 then surface orientation can be determined to ±6.8° of its true value. This corresponds to an area of gradient space in the third quadrant where the error regions are small. Here, a measurement error of 1 gray level in 10 in each of $I_1(x,y)$ and
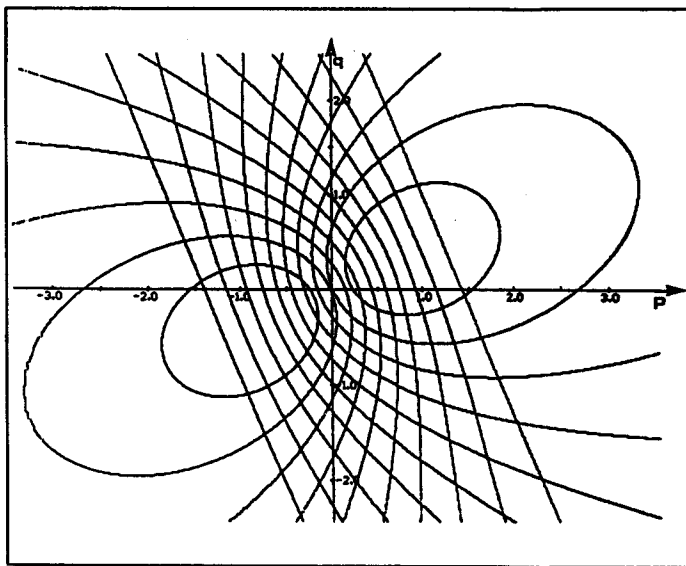
Figure 9. Superimposed reflectance maps $R_1(p,q)$ and $R_2(p,q)$ where $R_1(p,q)$ is $R_a(p,q)$ with $p_s = 0.7$, $q_s = 0.3$, $\varrho = 1$ and $R_2(p,q)$ is $R_a(p,q)$ with $p_s = -0.7$, $q_s = -0.3$, $\varrho = 1$. Each region indicates how an error in intensity measurement determines a corresponding error in the estimation of surface gradient (p,q).

$I_2(x,y)$ constrains surface orientation to within $\pm 6.8°$. On the other hand, if $I_1(x,y)$ is determined to lie between 0.9 and 1.0 and $I_2(x,y)$ is determined to lie between 0.5 and 0.6 then surface orientation can be determined to $\pm 25.8°$ of its true value. This corresponds to an area of gradient space in the first quadrant where the error regions are large. Here, a measurement error of 1 gray level in 10 in each of $I_1(x,y)$ and $I_2(x,y)$ only constrains surface orientation to within $\pm 25.8°$.

Figure 9 repeats the example of Figure 8 but with the second light source separated by 180° in azimuth from the first. In this configuration, error regions are smallest in the second and fourth quadrants of gradient space. Combinations using more than two light sources can be arranged to achieve a desired overall accuracy. One idea is to choose four directions of illumination, spaced evenly in azimuth with respect to the viewer and having a relatively large phase angle g.[13] In such a configuration, most points of interest are illuminated by at least three independent sources and contours can be selected to intersect which are nearly perpendicular and where error regions are small.

CONCLUSIONS

Surface orientation can be determined from the image intensities obtained under a fixed imaging geometry but with varying lighting conditions. Photometric methods for determining surface orientation can be considered complementary to methods based on the identification of corresponding points in two images taken from different viewpoints:

1. Traditional stereo allows the accurate determination of distances to objects. Photometric stereo is best when the surface gradient is to be found.
2. Traditional stereo works well on rough surfaces with discontinuities in surface orientation. Photometric stereo works best on smooth surfaces with few discontinuities.
3. Traditional stereo works well on textured surfaces with varying surface reflectance. Photometric stereo is best when applied to surfaces with uniform surface properties.

Photometric stereo does have some unique advantages:
1. Since the images are obtained from the same point of view, there is no difficulty identifying corresponding points in the two images. This is the major computational task in traditional stereo.
2. Under appropriate circumstances, the surface reflectance factor can be found because the effect of surface orientation on image intensity can be removed. Traditional stereo provides no such capability.
3. Describing object shape in terms of surface orientation is preferable in a number of situations to description in terms of range or altitude above a reference plane.

Photometric stereo depends on a detailed understanding of the imaging process. In addition, the imaging instrument must be of high caliber so that the gray levels produced can be dependably related to scene radiance. Fortunately, our understanding of image formation and the physics of light reflection has advanced sufficiently, and the quality of imaging devices is now high enough, to make this endeavor feasible.

ACKNOWLEDGMENTS

REFERENCES

1. Nicodemus, F. E., Richmond, J. C. and Hisa, J. J., "Geometrical considerations and nomenclature for reflectance," NBS Monograph 160, National Bureau of Standards, Washington, D. C., 1977.
2. Mackworth, A. K., "Interpreting pictures of polyhedral scenes," Artificial Intelligence, Vol. 4, pp. 121-137, 1973.
3. Horn, B. K. P., "Understanding image intensities," Artificial Intelligence, Vol. 8, pp. 201-231, 1977.
4. Horn, B. K. P. and Sjoberg, R. W., "Calculating the reflectance map," Applied Optics, Vol. 18, No. 11, pp. 1770-1779, 1979.
5. Horn, B. K. P., "Automatic hill-shading using the reflectance map," Proc. Image Understanding Workshop, Palo Alto, California, April 1979.
6. Strat, T. M., "Shaded perspective images of terrain," TR-463, M.I.T. A.I. Laboratory, Cambridge, Mass., 1978.
7. Horn, B. K. P. and Bachman, B. L., "Using synthetic images to register real images with surface models," Comm. ACM, Vol. 21, No. 11, pp. 914-924, 1978.
8. Horn, B. K. P., "Obtaining shape from shading information," The Psychology of Computer Vision, P. H. Winston (ed.), McGraw-Hill, pp. 115-155, 1975.
9. Rindfleisch, T., "Photometric method for lunar topography," Photogrammetric Engineering, Vol. 32, pp. 262-276, 1966.
10. Woodham, R. J., "A cooperative algorithm for determining surface orientation from a single view," Proc. IJCAI-77, pp. 635-641, Cambridge, Mass., 1977.
11. Huffman, D. A., "Curvature and creases: a primer on paper," Proc. Conf. Computer Graphics, Pattern Recognition and Data Structures, IEEE Pub. 75CH0981-1C, pp. 360-370, 1975.
12. Woodham, R. J., "Relating properties of surface curvature to image intensity," Proc. IJCAI-79, pp. 971-977, Tokyo, Japan, 1979.
13. Woodham, R. J., "Reflectance map techniques for analyzing surface defects in metal castings," TR-457, M.I.T. A.I. Laboratory, Cambridge, Mass., 1978.
14. Horn, B. K. P., "Three source photometry," (personal communication), 1978.
15. Ikeuchi, K. and Horn, B. K. P., "An application of the photometric stereo method," Proc. IJCAI-79, pp. 413-415, Tokyo, Japan, 1979. s